Neoplasia 49 (2024) 100971

Contents lists available at ScienceDirect

Neoplasia

journal homepage: www.elsevier.com/locate/neo

Original Research

Reciprocal regulation of lncRNA MEF and c-Myc drives colorectal cancer tumorigenesis

Shuang Wu [a,1], Xiangyu Dai [a,b,4], Zhipu Zhu [b,1], Dianhui Fan [a], Su Jiang [1], Yi Dong [b], Bing Chen [b], Qi Xie [b], Zhihui Yao [b], Qun Li [a], Rick Francis Thorne [b], Yao Lu [c,*], Hao Gu [a,*], Wanglai Hu [a,b,*]

[a] Department of Immunology, School of Basic Medical Sciences, Anhui Medical University, Hefei 230027, China
[b] Translational Research Institute, People's Hospital of Zhengzhou University, Academy of Medical Science, Henan International Joint Laboratory of Non-coding RNA and Metabolism in Cancer, Tianjian Laboratory of Advanced Biomedical Sciences, State Key Laboratory of Esophageal Cancer Prevention and Treatment, Zhengzhou University, Zhengzhou, 450003, China
[c] Department of Anesthesiology, the First Affiliated of Anhui Medical University, Anhui Medical University, Hefei 230022, China

ARTICLE INFO

Keywords:
c-Myc
lncRNA-MEF
hnRNPK
TRIM25
Colorectal cancer

ABSTRACT

More than half of all cancers demonstrate aberrant c-Myc expression, making this arguably the most important human oncogene. Deregulated long non-coding RNAs (lncRNAs) are also commonly implicated in tumorigenesis, and some limited examples have been established where lncRNAs act as biological tuners of c-Myc expression and activity. Here, we demonstrate that the lncRNA denoted c-Myc Enhancing Factor (MEF) enjoys a cooperative relationship with c-Myc, both as a transcriptional target and driver of c-Myc expression. Mechanistically, MEF functions by binding to and stabilizing the expression of hnRNPK in colorectal cancer cells. The MEF-hnRNPK interaction serves to disrupt binding between hnRNPK and the E3 ubiquitin ligase TRIM25, which attenuates TRIM25-dependent hnRNPK ubiquitination and proteasomal destruction. In turn, the stabilization of hnRNPK through MEF enhances c-Myc expression by augmenting the translation c-Myc. Moreover, modulating the expression of MEF in shRNA-mediated knockdown and overexpression studies revealed that MEF expression is essential for colorectal cancer cell proliferation and survival, both in vitro and in vivo. From the clinical perspective, we show that MEF expression is differentially increased in colorectal cancer tissues compared to normal adjacent tissues. Further, correlations exist between MEF, c-Myc, and hnRNPK suggesting the MEF-c-Myc positive feedback loop is active in patients. Together these data demonstrate that MEF is a pivotal partner of the c-Myc network and propose MEF as a valuable therapeutic target for colorectal cancer.

Introduction

The protooncogene c-Myc is a dominant driver of tumorigenesis and represents one of the most promising cancer therapeutic targets [1]. Fundamentally a transcription factor, c-Myc has been shown to control 10 to 15 % of genes in the human genome and is also suggested to be a global amplifier of active promoters [2]. Importantly, c-Myc is aberrantly activated in ~40 % of all human cancers, variously resulting from gene amplification, chromosomal translocations or by upstream growth factor signaling [3,4]. Despite arising through heterogeneous mechanisms, c-Myc up-regulation and/or activation occurs in the large majority of certain cancer types, for example, in up to 70 % of cases colorectal cancer (CRC) [5,6]. As such, c-Myc upregulation contributes to the cancer initiation and development through controlling the cell cycle and proliferation, along with variety of diverse cellular events ranging from metabolism to apoptosis [3,7,8]. Considering the significant contribution of c-Myc to oncogenesis, its expression and activity must be strictly regulated where a variety of transcriptional and

Abbreviation: lncRNA, long noncoding RNA; CRC, colorectal cancer; CCAT1, colon cancer associated transcript; CCAL, colorectal cancer-associated lncRNA; IDH1-AS1, isocitrate dehydrogenase 1 antisense RNA1; EPIC1, epigenetically induced lnCRNA1; MILNR1, c-Myc interacting long non-coding RNA 1; Fbxw7, F-box and WD repeat domain containing 7; ISH, in situ hybridization; hnRNPK, heterogeneous nuclear ribonucleoprotein K; TRIM25, tripartite motif containing 25; BR, binding regions; RIP, RNA immunoprecipitation; ChIP, chromatin immunoprecipitation; IHC, immunohistochemistry; CHX, cycloheximide.

* Corresponding Authors.
E-mail addresses: yaolu@hmu.edu.cn (Y. Lu), guhao@ahmu.edu.cn (H. Gu), wanglaihu@ahmu.edu.cn (W. Hu).

[1] These authors contributed equally to this work

https://doi.org/10.1016/j.neo.2024.100971
Received 23 August 2023; Received in revised form 9 January 2024; Accepted 9 January 2024

posttranscriptional mechanisms have been identified [9]. Notably, c-Myc expression is essential for the activities of normal cells albeit at relatively low levels compared to the aberrantly high levels observed in cancer cells [10,11]. Consequently, one of the main difficulties in targeting c-Myc is the need to spare its expression in normal cells while achieving sufficient antagonistic effects in cancer cells.

Other important players involved in the development and progression of a variety of human cancers are long noncoding RNAs (lncRNAs)

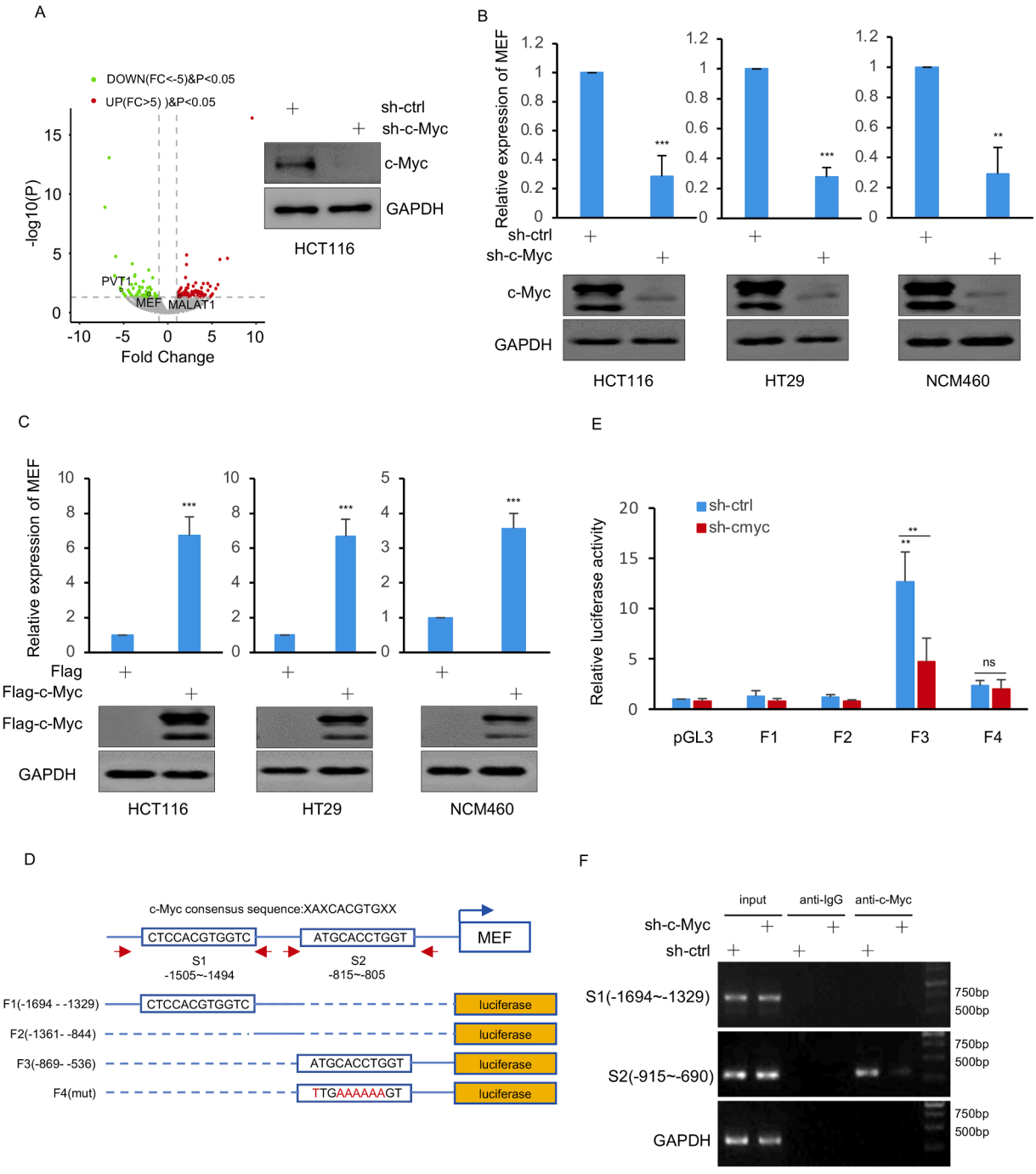

Fig. 1. MEF expression is transcriptionally regulated by c-Myc. A. Volcano plot derived from RNA sequencing analysis of HCT116 cells showing differentially regulated lncRNA transcripts between control (shRNA-ctrl) and c-Myc-targeting (shRNA-c-Myc) shRNAs. MEF is highlighted as a c-Myc responsive lncRNA along with the previously identified lncRNAs, PVT1 and MALAT1. The knockdown of c-Myc was verified by Western blotting as shown in the inset. GAPDH was used as an internal loading control throughout. B. The expression of MEF (top) and c-Myc (bottom) in the colorectal cancer cell lines HCT116, HT29 and normal NCM460 colon cells after transduction with shRNA-ctrl or shRNA-c-Myc as determined by qPCR and Western blot, respectively. C. MEF (top) and c-Myc (bottom) expression was evaluated as per (B) after transduction of cells with control vector or flag-c-Myc. D. Schematic diagram of two putative sites (S1 and S2) identified in the MEF proximal promoter conforming to the c-Myc consensus binding sequence (xAxCACGTGxx) (top). Based on these sites, pGL3-based reporter vectors were constructed (F1, F2 and F3) to evaluate c-Myc binding activity using luciferase assays (bottom). Primer pairs used to test c-Myc binding of the S1 and S2 sites in ChIP assays are shown by the red facing arrows. E. HCT116 cells stably expressing shRNA-ctrl or shRNA-c-Myc were transfected for 24 h with the indicated pGL3-based luciferase reporter constructs from (D) along with Renila luciferase and normalized reporter activity determined. F. ChIP assays were conducted in HCT116 cells using anti-c-Myc antibodies or IgG. S1 and S2 ChIP products for MEF along with GAPDH as a negative control were amplified by semi-quantitative RT-PCR.

[12,13]. Various studies have now shown that the dysregulation of lncRNAs also represents an important driver of cancer initiation and progression [14]. In CRC for example, CCAT1 (colon cancer associated transcript 1) induces cancer development via targeting BRD4, whereas CCAT2 and CCAL (colorectal cancer-associated lncRNA) promote CRC metastasis process through the Wnt signaling pathway [15–17]. Moreover, there is increasing appreciation that the oncogenic activities of c-Myc arise through the aberrant functioning of lncRNAs, albeit through different regulatory modalities.

First, lncRNAs are among the diverse targets of c-Myc and notably, the list of lncRNAs regulated by c-Myc in cancer cells is rapidly expanding [18]. For example, the direct c-Myc transcriptional target lncRNA EMS (E2F1 mRNA stabilizing factor) promotes tumor growth by increasing E2F1 expression [19] while alternatively c-Myc also suppresses the expression of lncRNA IDH1-AS1 (isocitrate dehydrogenase 1 antisense RNA1) to restrain cancer growth through regulating the Warburg effect [20]. Secondly, lncRNAs are not only targets but they also act as important functional partners of c-Myc. For instance, EPIC1 (epigenetically induced lnCRNA1) binds to c-Myc protein to enhance c-Myc occupancy at target gene promoters [21]. We have also found that MILNR1 (c-Myc interacting long non-coding RNA 1) inhibits c-Myc transcriptional activity via interactions in cis [22]. Thirdly, the expression of c-Myc can also be controlled by lncRNAs, as occurs with lncRNA MIF (c-Myc inhibitory factor) that induces c-Myc degradation by increasing the expression of Fbxw7 (F-box and WD repeat domain containing 7), a well-known E3 ubiquitin ligase that targets c-Myc. Nevertheless, the vast majority of lncRNAs in the human genome remain functionally uncharacterized, and it can be predicted that many linkages exist between lncRNAs and c-Myc that remain to be discovered.

Here, we identify the essential involvement of a lncRNA we call c-Myc Enhancing Factor (MEF) in c-Myc's regulatory network in colorectal cancer cells. MEF was identified as part of a screen to identify novel c-Myc-driven lncRNAs but our further mechanistic studies revealed MEF is more than a downstream target. Rather, we identified that MEF is involved in a positive feedback loop with c-Myc that converges on hnRNPK. MEF fundamentally contributes to maintaining hnRNPK levels through direct binding which disrupts interactions between the E3 ligase TRIM25 and hnRNPK and stabilizing hnRNPK further reinforces c-Myc levels through translational increases. Moreover, we show that MEF is commonly upregulated in colorectal cancer tissues and is critical for colorectal cancer cell proliferation and survival, proposing MEF as a potentially valuable therapeutic target.

Results

1. Identification of MEF as a c-Myc transactivated lncRNA in colorectal cancer

Given the important role of aberrant c-Myc activation in CRC [23] and the contributions of lncRNAs to cancer progression, we hypothesized that identifying c-Myc-responsive lncRNAs would provide new insights into CRC pathogenesis. Towards this, we undertook comparative RNA profiling of HCT116 CRC cells bearing control or c-Myc knockdown shRNAs (Fig. 1A). To validate this analysis, we used qPCR to confirm that five selected lncRNA hits were indeed responsive to c-Myc knockdown along with the previously reported lncRNA PVT1 (supplementary Fig. 1A) [24]. Notably, knockdown of lncRNA NR-051976, but not other lncRNAs, led to significantly reduced cell proliferation in HCT116 cells (supplementary Fig. 1B). Thus, we chose to focus on lncRNA NR-051976 for further verification and analysis. And for reasons disclosed in the following experiments, we designate this lncRNA as MEF (c-Myc Enhancing Factor) given its function in enhancing c-Myc expression.

To first verify the relationship between c-Myc and MEF expression, we extended our analysis to additional cell lines. Indeed, the depletion of c-Myc in HCT116 and HT29 CRC cells and NCM460 normal colon cells resulted in decreased levels of MEF (Fig. 1B). Conversely, ectopic c-Myc expression increased MEF levels in all three cell lines (Fig. 1C). We next sought to understand the underlying mechanism of how MEF is regulated in response to c-Myc levels. Bioinformatics interrogation of the promoter of *MEF* revealed two consensus binding regions (BRs) for c-Myc (-1505/-1494 and -815/-805, respectively). Luciferase-based transcriptional reporters designed to test the activity of the two BRs (Fig. 1D) showed that only the S2 region proximal to the TSS was responsive to c-Myc whereas S1 was not active. Instructively, mutation of the BR within the S2 region ablated the responsiveness of the reporter to c-Myc expression (Fig. 1E). Furthermore, the direct binding of endogenous c-Myc to the S2 region was confirmed by ChIP assays, with binding being significantly impaired by knockdown of c-Myc (Fig. 1F). Taken together, these findings indicate that MEF expression is transcriptionally controlled by c-Myc.

2. Elevated MEF expression levels in colorectal cancer cells is critical for their proliferation

To elucidate whether MEF likely contributes to CRC pathogenesis, we first analyzed 40 paired human CRC samples. Notably, qPCR analyses indicated that CRC lesions displayed relatively higher levels of MEF compared to their corresponding normal adjacent tissues (Fig. 2A and B). Similarly, in situ hybridization (ISH) analysis of HCT116, HT29 and NCM460 normal colonic cells demonstrated relatively higher expression of MEF in colorectal cancer cell lines compared to normal cells (Fig. 2C). These data demonstrate that MEF is overexpressed in CRC lesions and cell lines, implying that aberrant MEF expression may play important role in human CRC development and/or progression.

To next delineate the function of MEF in CRC, we silenced MEF in the HCT116 and HT29 cell lines using two independent shRNAs to evaluate for off-target effects (Fig. 2D). Indeed, depletion of MEF induced striking inhibition of proliferation in both cell lines (Fig. 2E) while EdU incorporation assays showed that the proliferative capacity of HCT116 cells was remarkably inhibited by MEF knockdown (Fig. 2F). In addition, cell cycle assays showed that HCT116 cells with MEF depletion displayed significant increases in cell cycle arrest in the G1-phase (Fig. 2G). Moreover, the effects of MEF on cell viability and proliferation were mirrored in long-term survival using clonogenic assays (Fig. 2H). Additionally, depletion of MEF resulted in marked retardation of the in vivo growth of xenografted HCT116 tumors implanted in nu/nu mice (Fig. 2I and J). Collectively, these data support the notion that MEF is essential for CRC cell survival and proliferation, further proposing MEF functions as an oncogenic lncRNA.

3. MEF functions to stabilize hnRNPK protein levels through TRIM25

To dissect out the underlying molecular mechanisms responsible for the pro-survival activity of MEF, we hypothesized that, like many other regulatory lncRNAs, MEF acts through direct binding to protein effectors [22,25]. Of note, mass spectrometry analysis after RNA-pulldown assays against MEF identified hnRNPK (heterogeneous nuclear ribonucleoprotein K) and TRIM25 (tripartite motif containing 25) as candidate MEF binding proteins (Fig. 3A). The association between MEF, hnRNPK and TRIM25 was subsequently verified by Western blotting (Fig. 3B). Further analysis showed that depletion of MEF triggered marked reduction in the protein levels of hnRNPK, which was attributable to proteasomal degradation since hnRNPK levels were stabilized by MG132. However, although MEF bound to TRIM25, the levels of TRIM25 were not affected by MEF knockdown (Fig. 3C). These results suggested that MEF influences the protein stability of hnRNPK but not TRIM25.

TRIM25 belongs to the TRIM family whose members predominately function as both E3 ubiquitin ligases and RNA-binding proteins [26–28]. We therefore considered if TRIM25 was involved in the MEF-mediated regulation of hnRNPK. Instructively, the depletion of TRIM25 resulted in increased hnRNPK levels, and the effects of MEF knockdown in HCT116 cells were largely diminished when both TRIM25 and MEF were co-depleted (Fig. 3D), suggesting that the proteasomal effects of MEF on hnRNPK were dependent upon TRIM25. Consistently, the silencing or overexpression of MEF resulted in respective increases and

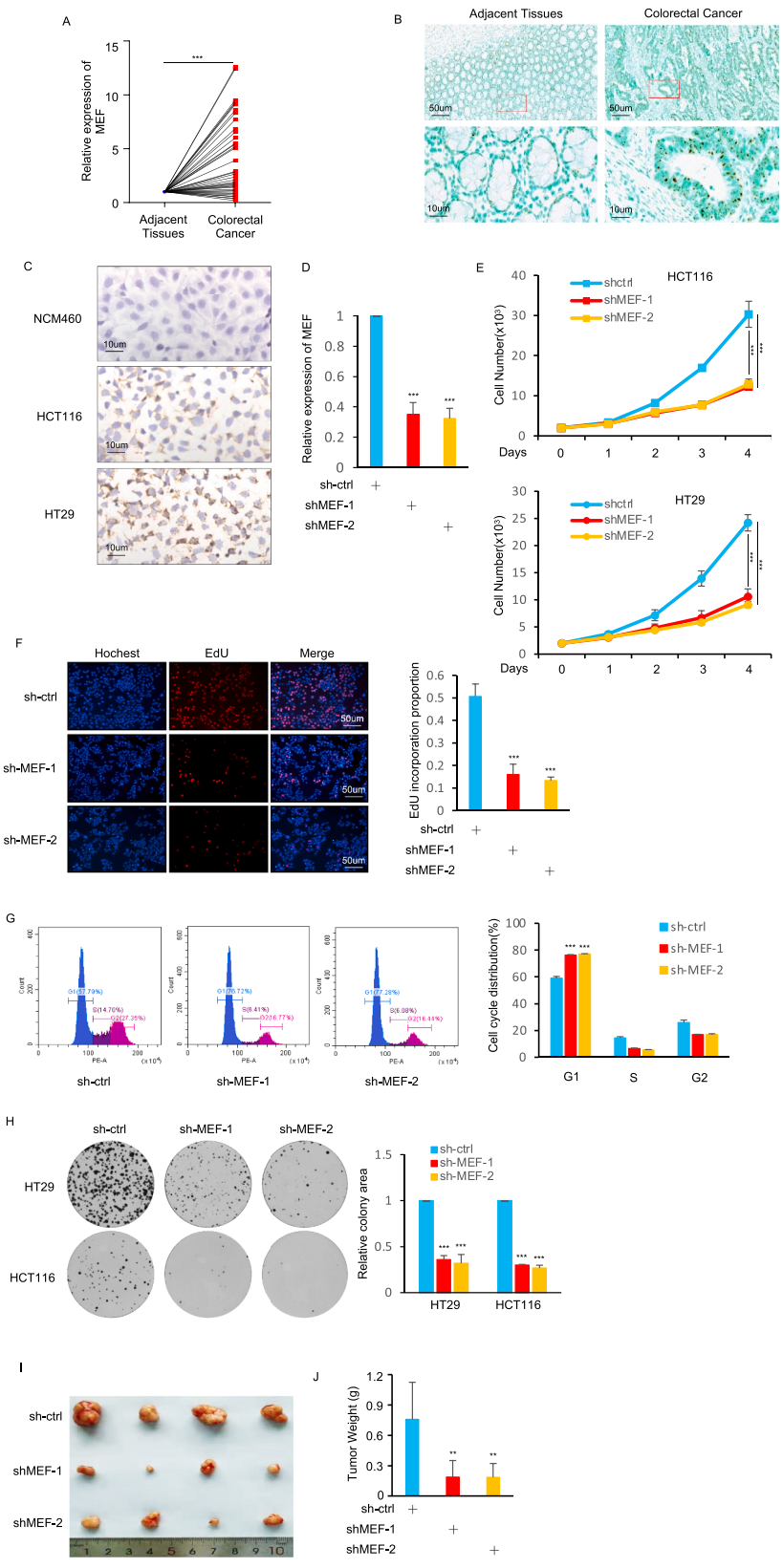

(caption on next page)

Fig. 2. MEF is essential for colorectal cancer cell survival and proliferation. A. Relative expression levels of MEF were examined using qRT-PCR in a cohort of 40 pairs of colorectal cancer and adjacent normal tissues. B. Representative images of in situ hybridization (ISH) detecting MEF expression in the colorectal cancer cohort from (A). C. ISH analysis of MEF expression in colorectal cancer cell lines (HCT116, HT29) and normal NCM460 colon cells. D. Representative qPCR assay demonstrating MEF knockdown efficiency of two independent MEF-targeting shRNAs (shRNA-MEF-1 or -2) compared to the shRNA-ctrl in HCT116 cells. E. Cell proliferation rates of HCT116 and HT29 cells were compared over 4 consecutive days after knockdown of MEF using CCK-8 assays as per (D). F. EdU incorporation assays conducted in HCT116 cells with and without stable knockdown of MEF. Cell nuclei were counterstained with Hoechst 33342 and the results expressed as the ratio of EdU-positive cells to total Hoechst 33342-positive cells. G. Flow cytometric-based analysis of cell cycle parameters in HCT116 cells bearing shRNA-ctrl or shRNA-MEF. H. Long term growth of the HT29 and HCT116 cells from (E) assessed using clonogenic assays. I, J. HCT116 cells (2×10^6) stably expressing shRNA-ctrl or shRNA-MEF were injected s.c. into the flanks of nude mice (n = 6 for each group). Xenografts growth (I) and final tumor weights after dissection (J) were compared.

decreases, respectively, in the poly-ubiquitination of hnRNPK (Fig. 3E and F). As anticipated, MEF knockdown markedly increased the degradation of hnRNPK in cycloheximide chase assays (Fig. 3G), indicating reduced hnRNPK protein stability. However, the effects of MEF-knockdown on enhancing hnRNPK poly-ubiquitination and stabilizing hnRNPK protein levels, respectively, were nullified when TRIM25 was silenced (Fig. 3E and G). These findings indicated that MEF acts to prevent proteasomal degradation of hnRNPK in a TRIM25-dependent manner although the precise mechanism remained to be determined.

4. MEF stabilizes hnRNPK protein levels through disrupting TRIM25-hnRNPK interactions

Given that hnRNPK and TRIM25 were identified as MEF binding proteins, we hypothesized that MEF stabilizes hnRNPK in concert with binding to TRIM25. Indeed, RNA immunoprecipitation analysis showed that hnRNPK and TRIM25 interacted strongly with MEF in a fully reciprocal manner (Fig. 4A and B), suggesting their interactions serve to regulate hnRNPK levels. Nevertheless, these assays were unable to distinguish whether such regulation resulted from competitive binding events between MEF, hnRNPK and TRIM25 or otherwise interactions as part of a ternary complex. To distinguish between these possibilities, immunoprecipitation assays conducted after MEF knockdown revealed strongly enhanced binding between TRIM25 and hnRNPK (Fig. 4C). Consistently, binding assays conducted with in vitro synthesized MEF but not antisense MEF restrained the association between recombinant hnRNPK and TRIM25 (Fig. 4D). Furthermore, silencing of MEF selectively increased binding between hnRNPK and TRIM25 in a mammalian two-hybrid system (Fig. 4E). Thus, collectively these results propose that MEF acts to disassociate or prevent TRIM25 from binding to hnRNPK.

To further delineate the structural determinants underlying their respective interactions, we carried out deletion-mapping experiments. First, RNA-pulldown assays performed with in vitro transcribed MEF truncation mutants using an exon deleting strategy (Fig. 4F) showed that sequences within exon 1 (P1) supported the binding of MEF to both hnRNPK and TRIM25 (Fig. 4G and H). Moreover, the ectopic expression of MEF and also the P1 but not P2 construct, increased the half-life of hnRNPK (Fig. 4I), consistent with a regulatory model where MEF binding serves to disrupt the hnRNPK-TRIM25 association.

5. MEF enhances c-Myc translational efficiency through hnRNPK

We returned to consider the relationship between c-Myc and MEF, especially given that hnRNPK is known to be important for regulating the expression of c-Myc [29,30]. A logical experiment was therefore to test whether MEF influenced c-Myc expression via its regulatory effects on hnRNPK levels. Indeed, MEF knockdown reduced c-Myc protein levels which could otherwise be rescued by the ectopic expression of hnRNPK (Fig. 5A). The effects of MEF on c-Myc expression were independent of transcriptional processes as neither depletion nor ectopic expression of MEF influenced the levels of c-Myc mRNA (Fig. 5B and C) nor did these manipulations affect the degradation rate of c-Myc mRNA (Fig. 5D and E).

Based on these findings, we hypothesized that MEF regulates c-Myc expression through translation. Consequently, we performed polysome profiling to examine c-Myc mRNA translation levels in cells subjected to MEF knockdown or overexpression. Notably, these manipulations produced minimal effects on the ribosomal velocity sedimentation profiles (Fig. 5F and H), indicating there were no global perturbation of polysome assembly. However, MEF silencing decreased the levels of c-Myc mRNA associated with polysomes, whereas conversely, the overexpression of intact MEF or the P1 truncation mutant increased polysome-associated c-Myc mRNA levels (Fig. 5G and I). These findings together with our preceding data establish that MEF serves to enhance c-Myc protein expression through enhancing its translation via a hnRNPK-dependent mechanism.

6. A c-Myc-MEF positive feed-back loop contributes to CRC tumorigenesis

Collectively our data reveal the existence of a positive feedback loop between c-Myc and MEF but its overall significance regarding CRC tumorigenesis remained to be determined. As anticipated, MEF overexpression enhanced the rates of HCT116 cell proliferation and clonogenicity in vitro which was phenocopied by ectopic expression of the P1 truncation construct but not P2 (Fig. 6A and B). Similarly, the growth of HCT116 cell xenografts in nude mice was potentiated by MEF overexpression with increased tumor sizes also evident with P1 construct overexpressing cells but not with P2 (Fig. 6C). Thus, regulating the cellular expression levels of MEF significantly impacted key measures of CRC tumorigenesis in experimental models. Moreover, this activity was recapitulated by expressing only the MEF region responsible for binding to both hnRNPK and TRIM25.

Additionally, since elevated c-Myc expression induces genomic instability in tumor cells [31], we examined if MEF also contributes to changes in DNA integrity. However, using comet assays to assess DNA damage in HCT116 cells we found that MEF overexpression did not cause the appearance of DNA tails unlike the DNA damaging agent doxorubicin (supplementary Fig. 2A). Moreover, ectopic MEF expression failed to induce significant changes in the foci decorated by phosphorylated histone H2AX nor the levels of p53-binding protein 1 (53BP1), markers that represent the recruitment of DDR components to double-strand DNA breaks sites (supplementary Fig. 2B and C). These results suggest that MEF is not involved in altering genomic integrity in association with its regulatory relationship with c-Myc.

Finally, we analyzed associations between the expression of c-Myc, hnRNPK and MEF in colorectal cancer tissues to determine the likely importance of the c-Myc-MEF feed-back loop to the pathology of CRC. We divided our cohort of 40 colorectal cancer tissues into two groups, those with relatively low (<2 fold change, n = 18) and high (>2 fold change, n = 22) expression levels of MEF. In situ and immunohistochemistry analyses demonstrated that colorectal cancers with high MEF expression displayed significantly higher levels of c-Myc and hnRNPK, while low MEF expression was associated with less c-Myc and hnRNPK (Fig. 6D). Moreover, significant positive correlations were established between MEF and c-Myc, hnRNPK and MEF, and c-Myc and hnRNPK (Fig. 6E), proposing the existence of the c-Myc-MEF feed-back loop in CRC (Fig. 6F).

Discussion

Given its status as the most frequently deregulated oncogene in human cancer, c-Myc constitutes an attractive therapeutic target [32, 33]. However, transcription factors make notoriously difficult targets for small molecule inhibition approaches, prompting the search for alternative ways to counteract c-Myc signaling. And given the important

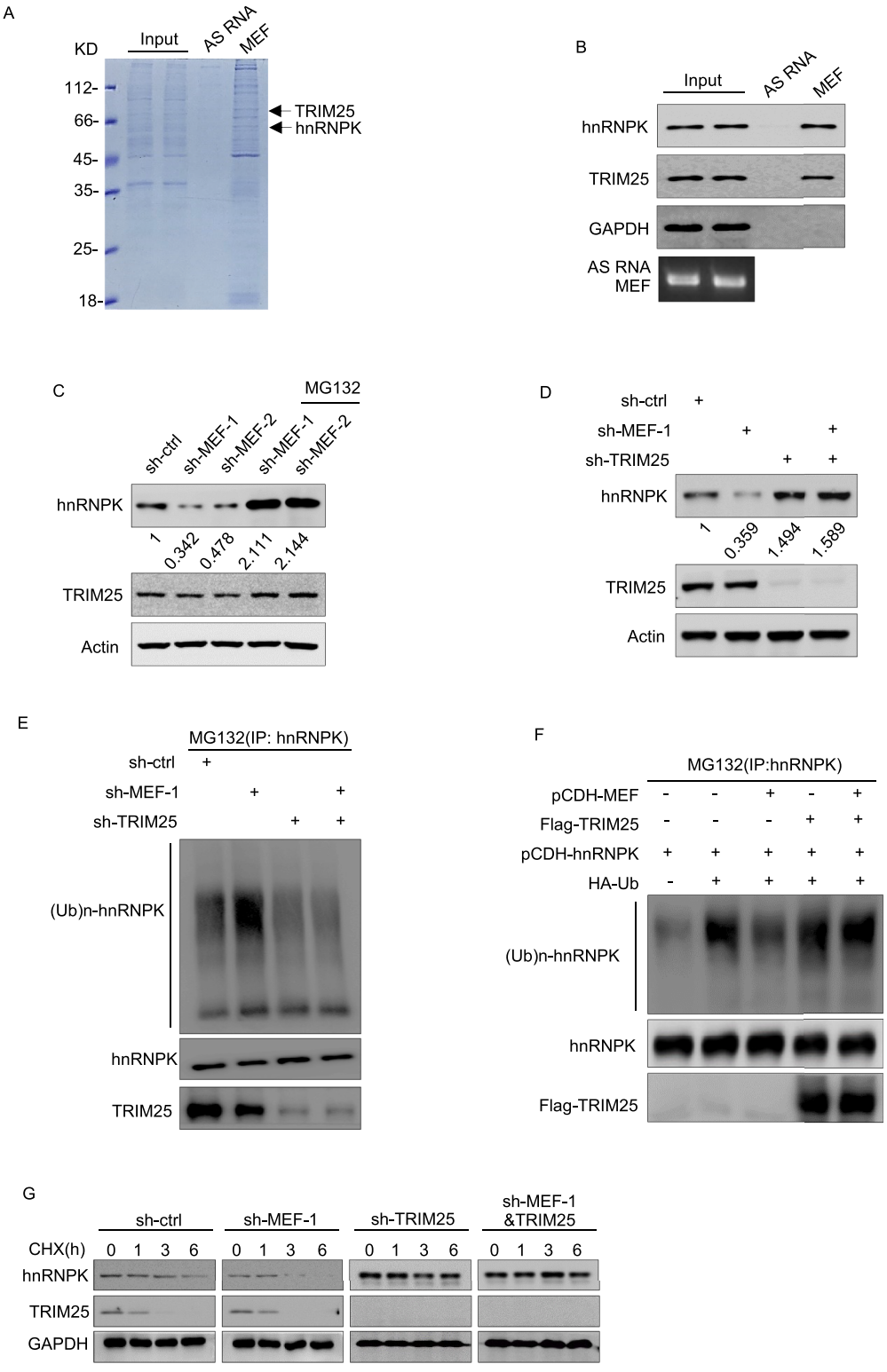

Fig. 3. MEF stabilizes hnRNPK protein levels through inhibiting its proteasomal degradation via TRIM25. A. RNA pull-down assays were conducted in HCT116 cells using in vitro synthesized sense or anti-sense MEF. Interrogation of specific bands by mass spectrometry identified hnRNPK and TRIM25 as candidate MEF interacting proteins. B. The selective interactions between hnRNPK and TRIM25 with MEF in the RNA pulldown samples from (A) were confirmed by Western blotting analysis. GAPDH was used as a negative control. C. HCT116 cells infected with the shRNA-control or shRNA-MEF-1 or -2 were treated with or without MG132 (10 μM) for 6 h. The levels of hnRNPK and TRIM25 were compared by Western blot. D. HCT116 cells were transfected with shRNA-MEF-1 alone or in combination with shRNA-TRIM25. The levels of hnRNPK and TRIM25 were analyzed by using Western blotting. E. HCT116 cells transfected as per (D) were treated with MG132 (10 μM) for 6 h before conducting immunoprecipitations against hnRNPK and Western blotting against ubiquitin (Ub), hnRNPK and TRIM25. F. HCT116 cells were co-transfected with the indicated combinations of hnRNPK and epitope labelled Flag-TRIM25 and HA-Ub before analysis of whole cell lysates as per (E). G. HCT116 cells stably expressing shRNA-MEF-1, shRNA-TRIM25 or both were treated with cycloheximide (50 μg/ml) for the indicated times and cell lysates were subjected to Western blot analysis with the indicated antibodies.

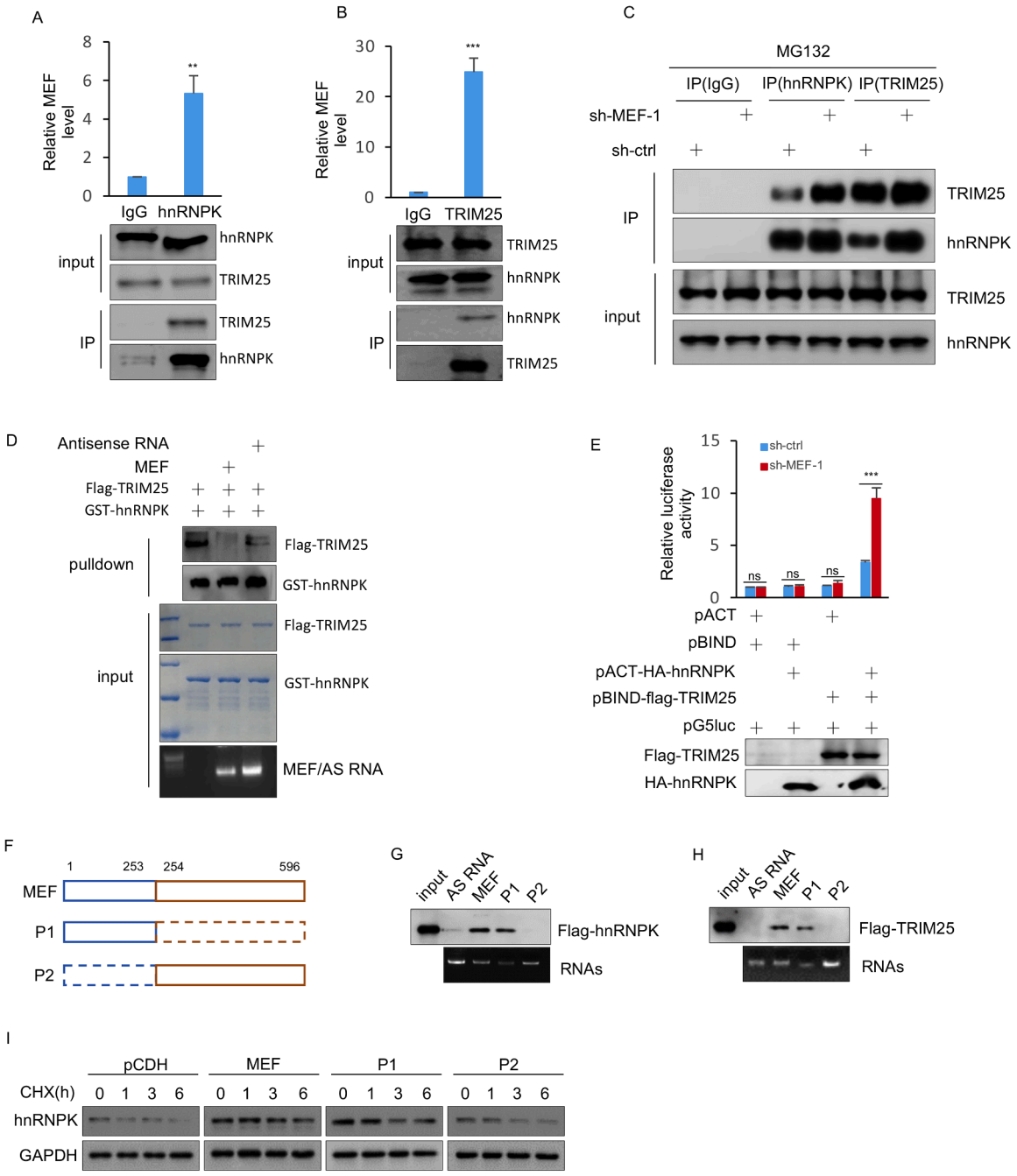

Fig. 4. MEF disrupts TRIM25-hnRNPK interactions to stabilize hnRNPK protein levels. A. RNA immunoprecipitation assays were performed using HCT116 cells against hnRNPK or using an isotype-matched IgG control. Immunoprecipitates were analyzed by qPCR and Western blotting, respectively to detect MEF or hnRNPK and TRIM25. B. RIP assays were conducted as per (A) using antibodies against TRIM25. C. HCT116 cells bearing shRNA-ctrl or shRNA-MEF-1 were treated with MG132 (10 μM) for 6 h. Cell lysates were immunoprecipitated using anti-hnRNPK, anti-TRIM15 or IgG control respectively before analyzing the precipitates by Western blotting with the indicated antibodies. D. GST-tagged hnRNPK adsorbed to glutathione agarose beads was incubated with purified recombinant Flag-TRIM25 in the presence of in vitro-transcribed MEF or MEF antisense RNA. The beads were then eluted, and samples analyzed by Western blot. E. Mammalian 2-hybrid assays were performed to evaluate interactions between hnRNPK and TRIM25. The indicated combinations of pBIND/pACT-based constructs were co-transfected into HCT116 cells bearing shRNA-ctrl or shRNA-MEF-1 for 24 h before measuring relative luciferase activity. Ectopic expression of hnRNPK and TRIM25 were confirmed by Western blotting (bottom). F. Schematic illustrating the design of truncated MEF constructs corresponding to individual exons of the MEF transcript (P1, 1-253 nt; P2, 254-596 nt). G. RNA pull-down assays were conducted with biotin-labelled sense or anti-sense MEF, P1 or P2 against cell lysates from 293T cells transfected with Flag-tagged hnRNPK. Co-precipitated proteins were analyzed by Western blot using anti-Flag antibodies. H. 293T cells transfected with Flag-tagged TRIM25 were subjected to RNA pulldown analysis as per (G). I. HCT116 cells bearing empty pCDH vector, pCDH-MEF, pCDH-P1 or pCDH-P2 were treated with cycloheximide (50 μg/ml) for the indicated times and the cell lysates analyzed by Western blotting.

contributions of lncRNAs in cancer, identifying functional intersections between lncRNAs and c-Myc offers potential therapeutic opportunities as well as providing new insights into tumorigenesis [34]. Here using a strategy to identify c-Myc-responsive lncRNAs, we discovered that a previously uncharacterized lncRNA we term MEF is critical for the cell survival and proliferation of colorectal cancer cells. The functional

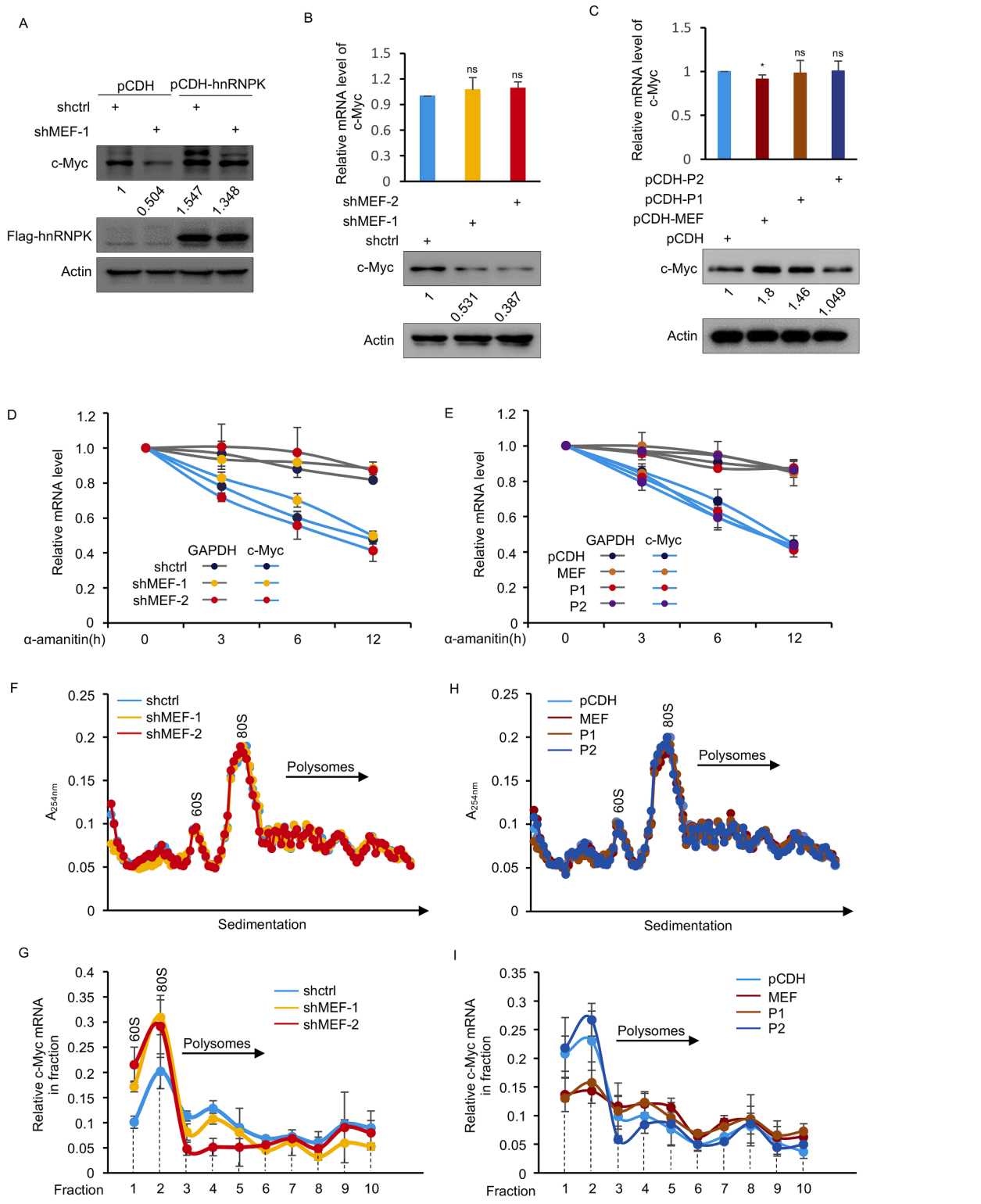

Fig. 5. MEF enhances c-Myc translational efficiency via hnRNPK. A. HCT116 cells bearing shRNA-ctrl or shRNA-MEF-1 were transfected with either control or Flag-hnRNPK expression vectors before analysis of c-Myc protein levels by Western blot. B. c-Myc mRNA levels in HCT116 cells were determined by qPCR after infection with either shRNA-ctrl or shRNA-MEF lentiviral vectors. Corresponding changes in c-Myc protein levels were monitored by Western blotting. C. HCT116 cells were transfected with pCDH, pCDH-MEF, pCDH-P1 or pCDH-P2, then the mRNA and protein level of c-Myc were measured by qPCR and Western blotting, respectively. D. HCT116 cells bearing shRNA-ctrl or shRNA-MEF were subjected to α-amanitin (1 ug/ml) treatment for the indicated times before determining the levels of c-Myc mRNA by qPCR. GAPDH was used as a negative control. E. RNA stability assays using α-amanitin treatment were conducted as per (E) in HCT116 cells bearing ectopic expression of pCDH, pCDH-MEF, pCDH-P1 or pCDH-P2. F. Polysome profiling analyses were performed in HCT116 cells bearing shRNA-ctrl or independent shRNA-MEF constructs by velocity sedimentation ultracentrifugation. Peaks corresponding to 60S ribosomes, 80S monosome complex, along with the polysome-containing fractions containing are denoted. G. The abundance c-Myc mRNA in fractions from (F) were evaluated by qPCR and calculated as a percentage of the total in all fractions. H. Polysome profiling assays were conducted as per (F) in HCT116 cells bearing ectopic expression of pCDH, pCDH-MEF, pCDH-P1 or pCDH-P2. I. The relative abundance of c-Myc mRNA in the fractions from (H) were analyzed as per (G).

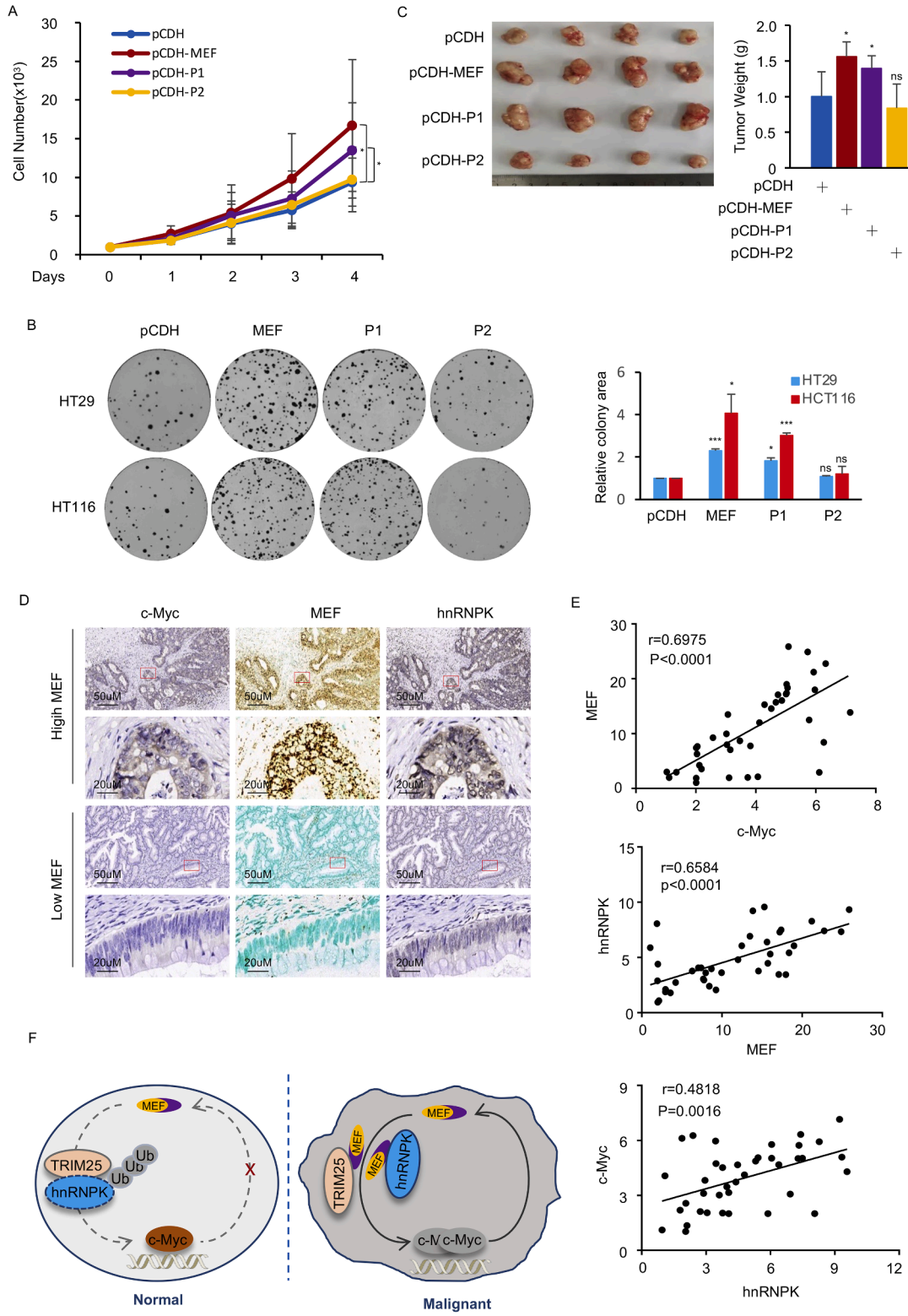

Fig. 6. MEF levels drive c-Myc expression and CRC tumorigenesis in vitro and in vivo. A. Cell proliferation rates were compared in HCT116 cells with ectopic expression of empty pCDH vector, pCDH-MEF, pCDH-P1 or pCDH-P2 using CCK-8 assays. B. Long term growth of the HT29 and HCT116 cells from (A) assessed using clonogenic assays. Assays were quantitated as shown in the right panel. C. HCT116 cells with ectopic expression of pCDH, pCDH-MEF, pCDH-P1 or pCDH-P2 were injected s.c. into the flanks of nude mice respectively (n = 6 for each group). Panels compare xenografts after dissection (left) and tumor weights (right). D. The cohort of 40 colorectal cancer tissues from Fig. 2B was subjected to further analysis to determine c-Myc and hnRNPK expression levels using IHC. The samples were divided into two groups according to MEF expression levels (low <2-fold change, n=18; high >2-fold change, n=22). The images show photomicrographs comparing the expression of c-Myc and hnRNPK in CRC and matched normal tissues from representative tissues with high and low MEF expression, respectively. E. Correlation analyses performed between the expression of MEF, c-Myc and hnRNPK in 40 colorectal cancer tissues. Pearson correlation coefficients (r) and p values are shown for the individual comparisons. F. Working model illustrating the positive feedback loop that exists between MEF and c-Myc in colorectal carcinoma cells.

contribution of MEF was confirmed through both overexpression and knockdown studies using in vitro and in vivo models. Moreover, we observed that the expression of MEF was significantly up-regulated in human colorectal cancer tissues and was positively correlated with c-Myc, implying that MEF contributes to tumorigenesis. Together these observations suggest that MEF is an important downstream player in c-Myc's oncogenic network.

Further functional analyses showed that the effects of MEF on colorectal cancer cells were mediated through its stabilization of hnRNPK, itself considered to be an oncogene in several cancer types [35]. We showed that silencing of MEF increased the association between hnRNPK and the E3 ligase TRIM25. Furthermore, as MEF binding to hnRNPK and TRIM25 involved sequences embedded in exon 1 of MEF, the logical inference was that MEF competitively binds to hnRNPK to prevent its association with TRIM25. In turn, blocking TRIM25 binding serves to reduce hnRNPK proteolytic turnover by preventing hnRNPK polyubiquitination. Thus, TRIM25 joins the list of ubiquitin E3 ligases known to control the degradation of hnRNPK which prominently include MDM2 and FBXW7 [36–39]. Notably, while our experiments suggest TRIM25 directly targets hnRNPK degradation, TRIM family members often function as heterodimers with other TRIM members [28,40], leaving open the possibility that another TRIM protein is responsible for hnRNPK ubiquitin modifications. Nevertheless, more functional studies are needed to address this issue.

Another important finding disclosed in our study involved the relationship between MEF and c-Myc. Not only was MEF shown to be under the transcriptional control of c-Myc but we also found that MEF enhanced the translation of c-Myc in a hnRNPK dependent manner (Fig. 6F). The existence of a lncRNA-mediated positive feedback loop is noteworthy because of the requirement for c-Myc expression to be tightly regulated through transcriptional and posttranscriptional mechanisms, particularly in normal cells [9,41]. Presently, other examples of lncRNAs embedded in feedback loops with c-Myc involve its negative regulation. For instance, the lncRNA GAS5 (growth arrest-specific transcript 5) cooperates with eIF4E (eukaryotic translation initiation factor 4E) to suppress c-Myc translation through direct binding with its mRNA in lymphoma cells [42]. A further example also in cancer cells involves the lncRNA-MIF, which like MEF is a transcriptional target of c-Myc [43]. However, lncRNA-MIF acts as a non-coding competing endogenous RNA (ceRNA), competing with miR-586 for Fbxw7 mRNA binding to increase Fbxw7 levels, serving to accelerate the Fbxw7-dependent degradation of c-Myc. Whether the MEF-c-Myc relationship is also important for non-transformed cells remains to be determined but the actions of MEF in the cancer context appears intriguing. Moreover, while the deregulation of c-Myc plays a central role in many cancer types [44,45], more work is required to clarify whether the actions of MEF extend beyond colorectal cancer to include other cancer types.

Lastly, decades of attempts to target c-Myc as cancer treatment have largely not been successful [32,46]. Indeed, it been suggested that c-Myc is inherently "undruggable" at least from the perspective of interfering with its transcriptional activity [47,48]. This has led the search for alternative strategies to treat Myc-addicted cancers [49] with our findings here suggesting that MEF may represent a promising therapeutic target. We established that MEF functions as an oncogenic regulator by mediating the cancer-promoting effects of c-Myc. Moreover, targeting MEF in an experimental setting appears an effective means to inhibit c-Myc expression, at least in colorectal cancer cells. We envisage that the identification of small molecules that block the interaction of MEF with hnRNPK and TRIM25 constitutes one potential avenue to explore. Furthermore, with the introduction of technologies such GapMers [50,51] together with the FDA approval of several siRNA-based drugs [52,53], the era of targeted RNA therapeutics has appeared to have now arrived. Therefore, the selective targeting of MEF using clinically appropriate means also may offer an alternative approach for cancer treatment.

Methods and materials

Cell culture and reagents

The NCM460 cell line was generously provided by Prof. Huabing Zhang (Anhui Medical University), HCT116, HT29 whereas HEK293T cells were obtained from the ATCC. All cell lines were cultured in DMEM containing 10 % fetal bovine serum and 1 % penicillin/streptomycin, and authenticated using short-tandem repeat profiling within the past three years. Cells were regularly tested and confirmed to be mycoplasma-negative, and maintained at 37 °C with 5 % CO2. Antibodies used were purchased from the indicated manufacturers listed in supplementary table 1. Primers and shRNAs used were obtained from TsingKe BioTech and their sequences are also listed in supplementary table 1.

Patient tissues

Specimens from patients who were diagnosed with colorectal cancer were collected from People's Hospital of Zhengzhou University and the First Affiliated Hospital of Anhui Medical University. Samples were obtained by surgical excision and stored at -80 °C. All the experiments using human tissues were compliant with relevant ethical regulations and were conducted under approvals from the Human Research Ethics Committees of Anhui Medical University (81220277).

RNA pull-down experiments

Assays were performed as previously described [54]. Briefly, cell lysates were prepared by ultrasonication in RIP buffer containing a protease inhibitor cocktail and RNase inhibitors. In vitro transcribed biotin-labelled RNA (5 μg) was then adsorbed to streptavidin beads before incubation with cell lysates at 4 ℃ for 4∼6 hours. After washing the beads, the samples were eluted before further analysis.

RNA immunoprecipitation

RIP was performed as described previously [54]. Briefly, cells were lysed in hypotonic buffer containing RNase inhibitors and DNase I before centrifugation. Thereafter, cell lysates were incubated with protein A/G beads coated with indicated antibodies at 4 ℃ for 4 hours. After washing with RIP wash buffer, the bead-associated immunocomplexes were subjected to western blotting and qPCR analysis.

Chromatin immunoprecipitation (ChIP) assay

ChIP assays were performed as previously described [55]. Bound DNA fragments were detected using real-time PCR using the indicated primers (supplementary table 1).

EdU incorporation assay

Assays were performed using the EdU cell proliferation assay kit (C0078S, Beyotime, China) according to the manufacturer's instructions. The indicated cells were incubated with 10 uM EdU for 2h, fixed in 4 % formaldehyde, washed with PBS and permeabilized in 0.5 % Triton X-100. Cells were then incubated with the Apollo fluorescent probe for 30 min at room temperature followed by washing with PBS containing 3 % BSA. Subsequently, nuclei were counterstained with Hoechst-33342 for 10 min at room temperature. EdU-incorporating cells were evaluated by epifluorescence microscopy (Olympus IX71, Japan).

Cell cycle analysis

Experiments were performed using the cell cycle analysis kit (BB-4104, Bestbio, China). Briefly, 1×10^6 log-phase cells were plated into 6

cm plates at 50 % confluency. fter overnight culture, the cells were fixed in ice-cold 70 % ethanol overnight at -20 °C before staining with propidium iodide and analysis by flow cytometry (Beckman CytoFLEX, USA).

Immunofluorescence

The indicated cells grown on glass coverslips were fixed with 4 % formaldehyde, permeabilized in 0.2 % Triton X-100, blocked with 5 % BSA, and then incubated overnight at 4 °C with the indicated primary antibodies. Antibody detection was performed with Coralite-488 or 594 conjugated secondary antibodies as required, and nuclei counterstained with DAPI before microscopic examination.

Comet assays

Assays were performed according to the manufacturer's introduction (Jiancheng, Nanjing, China). Briefly, the indicated cells were mixed with agarose on the assay slides and after solidification, the slides were immersed in the lysis solution for 2 hours at 4 ℃. Thereafter, the slides were placed in unwinding solution for 1 hour at room temperature before submersion in the lysing solution for 2 h. The slides were then electrophoresed in electrophoresis buffer at 25 V (adjusted to 300 mA) for 30 min, neutralized with Tris buffer before staining with PI and observation by epifluorescence microscopy (Leica Microsystems, Germany).

Xenograft model

The indicated cells were subcutaneously injected into the dorsal flank of 4-week-old nude mice (GemPharmatech, Nanjing, China). After 21 days, mice were sacrificed and tumors were excised and weighed. Studies on animals were conducted with approval from the Animal Research Ethics Committee of Anhui Medical University (LLSC20200763).

Cell proliferation and colony formation assays

Cell proliferation and viability was assessed as previously described using CCK-8 assays [56]. Alternatively, for the colony assays, cells were seeded into 6-well plates at a density of 1000 cells per well. After two weeks, cells were fixed with 10 % cold methanol for 5 min and stained with 0.005 % (m/v) crystal violet for 30 min at room temperature. After extensive washing, the colonies were photographed and the percentage of the area covered by stained cell colonies were examined using the ImageJ.

Immunohistochemistry (IHC) and in situ hybridization (ISH)

Serial formalin-fixed paraffin-embedding colorectal cancer tissue sections were used for IHC and ISH analysis. IHC was performed as previously described [57] while ISH assays were conducted using the RNAscope 2.5 HD Reagent-BROWN kit according to the manufacturer's instructions [58]. Briefly, FFPE sections were deparaffinized twice in xylene for 5 min at RT, followed by rehydration in graded alcohol solutions. Sections were then incubated with hydrogen peroxide for 10 min at RT and heated in target retrieval reagent to 100 °C for 20 min, followed by being treated with proteinase K. After washing, sections were incubated with hybridization buffer containing probes (Advanced Cell Diagnostics, #410221) at 40 °C for 3 hours, followed by hybridization with AMP1 to AMP6 respectively. After being washed, the sections were incubated with 3,3′-diaminobenzidine (DAB), and counterstaining was carried out using methyl green. The percentage of positive cells was estimated from 0 % to 100 %. The intensity of staining was judged on an arbitrary scale of 0 to 4 as previously described [59]. A reactive score was derived by multiplying the percentage of positive cells with staining intensity divided by 10.

RNA isolation and qPCR assay

Total RNA was extracted using TRIzol (Invitrogen, Carlsbad, CA, USA) and 1 ug of total RNA was used for reverse transcription into cDNA using the HiScript II Q RT SuperMix (Vazyme, Nanjing, China) following the manufacturer's instructions. RNA concentration and purity was measured by NanoDrop (Thermo Fisher Scientific, Waltham, MA, USA). Quantitative real-time PCR (qRT-PCR) was performed on a Light-Cycler96 Instrument (Roche, Basel, Switzerland) using AceQ qPCR SYBR green Master Mix (Vazyme). The qRT-PCR reaction was performed in a final volume of 20 μL reaction mixture, containing 10 μL of 2 × qPCR Master Mix, 8 μL of diluted cDNA (100ng/μL), 1 μL each of 10 μM forward and reverse primers (supplemental Table 1). The PCR program was as follows: preincubation at 95 °C for 300 s, followed by 40 cycles of amplification with 95 °C for 10 s and 60 °C for 60 s, and a melt cycle from 60 °C to 95 °C. PCR results were recorded as cycle threshold (Ct) and the $2-\Delta\Delta CT$ method was used to calculate the relative gene expression levels in comparison to the ACTIN housekeeping gene.

Western blotting

Western blotting was performed as described before using ECL detection [60]. Briefly, samples were boiled in SDS loading buffer before separation by SDS-PAGE and protein transferred to nitrocellulose membranes (Bio-Rad). Thereafter, membranes were incubated with the indicated antibodies (supplementary table 1).

RNA interference

Gene knockdown experiments were performed using lentiviral-mediated transduction of shRNAs as described previously [60]. Stably transduced cell lines were selected by using 1 μg/ml puromycin before assessing knockdown efficiency by western blot. Targeting sequences are shown in supplementary table 1.

In vitro transcription

DNA templates for transcription were generated by PCR from plasmids using a forward primer recognizing the 5′ T7 RNA polymerase promoter sequence. The amplicon was purified using the DNA Gel Extraction Kit and used for subsequent in vitro transcription. In vitro transcription was performed using the T7-Flash BiotinRNA Transcription Kit (with biotin) or TranscriptAid T7 High Yield Transcription Kit (without biotin) according to the manufacturer's instructions. RNA was subsequently purified by using phenol-chloroform. Primer sequences are shown in supplementary table 1.

Polysome profiling assay

Polysome profiling assays were performed as described before [61]. Briefly, HCT116 cells with indicated treatments were pre-treated with CHX (100 ug/mL) for 10 min at 37 °C, washed with ice-cold PBS buffer containing CHX (100 ug/ml), and lysed in polysome lysis buffer (5 mM tris-HCl (pH 7.5), 2.5 mM MgCl2, 1.5 mM KCl, 1 mM DTT, 0.5 % Triton X-100, 0.5 % sodium deoxycholate, 100 g/ml CHX, 100 U of RNase inhibitor, and protease inhibitor cocktail). Cell lysates were centrifuged at 14,000 rpm for 10 min at 4 °C to remove the nuclei and mitochondria and then ribosomal particles (60S large subunit, 80S monosome, and polysome) were layered onto 11 ml of 10 to 45 % sucrose density gradients and centrifuged in an SW-41Ti rotor at 40,000 rpm at 4 °C for 2 hours. 100 equal volume fractions were collected from the tube bottom and ribosome distribution was analyzed by measuring the optical density (OD) at 254 nm (A254) by UV photometry (Thermo). Total RNA from each fraction was isolated with Trizol and the transcript abundance

of c-Myc was determined by qPCR.

Recombinant protein purification

Flag-tagged TRIM25 expressed in 293T cells was purified using anti-Flag coated protein A/G beads. The immunoprecipitates were then eluted with 3xFlag peptides. GST-hnRNPK was purified from E.coli using glutathione Sepharose at 4 °C overnight.

Luciferase reporter and mammalian two-hybrid assays

Luciferase reporter assays were performed according to the manufacturer's instructions as described before [60]. Mammalian two-hybrid assays were performed using an assay kit according to the manufacturer's instructions as previously described [25]. Briefly, complementary DNAs for hnRNPK and TRIM25 were cloned into the pACT and pBIND vectors to generate fusion proteins. pACT-hnRNPK and pBIND-TRIM25 constructs were co-transfected with the pG5luc vector into cells as indicated. 48 hours after transfection, firefly and Renilla luciferase activity was measured using the Dual-Luciferase Reporter Assay System.

Reproducibility and statistical analysis

All experiments were repeated at least three times. Analysis was performed using Microsoft Excel and GraphPad Prism to assess differences between experimental groups. Statistical significance was defined by Student's t test and expressed as a p value. $P < 0.05$ were considered to be statistical significance.

Supplementary Figure 1 related to Figure 1.

A. Five identified lncRNAs along with the previously reported c-Myc-responsive lncRNA PVT1 from the RNA profiling screen were validated by qPCR.

B. Cell viability determined using MTT assays in HCT116 cells cultured for four days bearing the indicated shRNAs.

Supplementary Figure 2 related to Figure 6.

A. Comet assays conducted to assess DNA damage in HCT116 cells with or without MEF overexpression. Cell treatment with doxorubicin was included as a positive control to reveal DNA damage through the appearance of comet tails.

B. HCT116 cells with or without ectopic MEF expression were subjected to immunofluorescence staining to detect γH2A.X foci and 53BP1 accumulation, respectively.

C. The protein levels of γH2AX and 53BP1 were measured by Western blotting in HCT116 cells treated as per (B).

CRediT authorship contribution statement

Shuang Wu: Conceptualization, Investigation, Resources, Writing – original draft. **Xiangyu Dai:** Conceptualization, Investigation, Methodology. **Zhipu Zhu:** Investigation, Methodology, Resources, Software. **Dianhui Fan:** Formal analysis, Methodology, Resources, Software. **Su Jiang:** Formal analysis, Methodology, Resources, Software. **Yi Dong:** Methodology, Resources, Software. **Bing Chen:** Methodology, Resources, Software. **Qi Xie:** Formal analysis, Methodology, Software. **Zhihui Yao:** Methodology, Resources, Software. **Qun Li:** Formal analysis, Resources, Software, Supervision. **Rick Francis Thorne:** Methodology, Resources, Software, Writing – original draft, Writing – review & editing. **Yao Lu:** . **Hao Gu:** Conceptualization, Funding acquisition, Project administration, Writing – original draft, Writing – review & editing. **Wanglai Hu:** .

Declaration of competing interest

The authors declare no competing interests.

Acknowledgments

This work was supported by grants from the National Natural Science Foundation of China (82022054, 81972622, 82002968, 82372658) and Anhui Science Fund for Distinguished Young Scholars (2008085J36). The authors thank the support from the scientific research improvement project of Anhui medical university (2019xkjT003).

Supplementary materials

Supplementary material associated with this article can be found, in the online version, at doi:10.1016/j.neo.2024.100971.

References

[1] M. Gabay, Y.L. Li, D.W. Felsher, MYC Activation Is a Hallmark of Cancer Initiation and Maintenance, Csh Perspect. Med. 4 (2014).
[2] C.Y. Lin, J. Loven, P.B. Rahl, R.M. Paranal, C.B. Burge, J.E. Bradner, T.I. Lee, R. A. Young, Transcriptional amplification in tumor cells with elevated c-Myc, Cell 151 (2012) 56–67.
[3] C.V. Dang, MYC on the path to cancer, Cell 149 (2012) 22–35.
[4] D.M. Miller, S.D. Thomas, A. Islam, D. Muench, K. Sedoris, c-Myc and cancer metabolism, Clin. Cancer Res. 18 (2012) 5546–5553.
[5] D.M. Muzny, M.N. Bainbridge, K. Chang, H.H. Dinh, J.A. Drummond, G. Fowler, C. L. Kovar, L.R. Lewis, M.B. Morgan, I.F. Newsham, et al., Comprehensive molecular characterization of human colon and rectal cancer, Nature 487 (2012) 330–337.
[6] M. Elbadawy, T. Usui, H. Yamawaki, K. Sasaki, Emerging roles of C-Myc in cancer stem cell-related signaling and resistance to cancer chemotherapy: a potential therapeutic target against colorectal cancer, Int. J. Mol. Sci. 20 (2019).
[7] C.V. Dang, K.A. O'Donnell, K.I. Zeller, T. Nguyen, R.C. Osthus, F. Li, The c-Myc target gene network, Semin. Cancer Biol. 16 (2006) 253–264.
[8] P.A. Carroll, B.W. Freie, H. Mathsyaraja, R.N. Eisenman, The MYC transcription factor network: balancing metabolism, proliferation and oncogenesis, Front. Med.-Prc. 12 (2018) 412–425.
[9] D. Levens, You don't muck with MYC, Genes. Cancer 1 (2010) 547–554.
[10] Z.E. Stine, Z.E. Walton, B.J. Altman, A.L. Hsieh, C.V. Dang, MYC, metabolism, and cancer, Cancer Discov. 5 (2015) 1024–1039.
[11] R. Dhanasekaran, A. Deutzmann, W.D. Mahauad-Fernandez, A.S. Hansen, A. M. Gouw, D.W. Felsher, The MYC oncogene - the grand orchestrator of cancer growth and immune evasion, Nat. Rev. Clin. Oncol. 19 (2022) 23–36.
[12] A.M. Schmitt, H.Y. Chang, Long noncoding RNAs in cancer pathways, Cancer Cell 29 (2016) 452–463.
[13] M. Huarte, The emerging role of lncRNAs in cancer, Nat. Med. 21 (2015) 1253–1261.
[14] M. Guo, J. Zhang, Q. Liang, J. Zhu, Q. Wang, Z. Fang, Z. Songyang, Y. Xiong, Pan-cancer pseudogene RNA analysis reveals a regulatory network promoting cancer cell proliferation, Genome Instab. Dis. 4 (2023) 85–97.
[15] M.L. McCleland, K. Mesh, E. Lorenzana, V.S. Chopra, E. Segal, C. Watanabe, B. Haley, O. Mayba, M. Yaylaoglu, F. Gnad, et al., CCAT1 is an enhancer-templated RNA that predicts BET sensitivity in colorectal cancer, J. Clin. Invest. 126 (2016) 639–652.
[16] Y. Ma, Y. Yang, F. Wang, M.P. Moyer, Q. Wei, P. Zhang, Z. Yang, W. Liu, H. Zhang, N. Chen, et al., Long non-coding RNA CCAL regulates colorectal cancer progression by activating Wnt/β-catenin signalling pathway via suppression of activator protein 2α, Gut 65 (2016) 1494–1504.
[17] H. Ling, R. Spizzo, Y. Atlasi, M. Nicoloso, M. Shimizu, R.S. Redis, N. Nishida, R. Gafà, J. Song, Z. Guo, et al., CCAT2, a novel noncoding RNA mapping to 8q24, underlies metastatic progression and chromosomal instability in colon cancer, Genome Res. 23 (2013) 1446–1461.
[18] R. Tu, Z. Chen, Q. Bao, H. Liu, G. Qing, Crosstalk between oncogenic MYC and noncoding RNAs in cancer, Semin. Cancer Biol. 75 (2021) 62–71.
[19] C. Wang, Y. Yang, G. Zhang, J. Li, X. Wu, X. Ma, G. Shan, Y. Mei, Long noncoding RNA EMS connects c-Myc to cell cycle control and tumorigenesis, Proc. Natl. Acad. Sci. u S. a 116 (2019) 14620–14629.
[20] S. Xiang, H. Gu, L. Jin, R.F. Thorne, X.D. Zhang, M. Wu, LncRNA IDH1-AS1 links the functions of c-Myc and HIF1α via IDH1 to regulate the Warburg effect, Proc. Natl. Acad. Sci. u S. a 115 (2018) E1465–e1474.
[21] Z. Wang, B. Yang, M. Zhang, W. Guo, Z. Wu, Y. Wang, L. Jia, S. Li, W. Xie, D. Yang, lncRNA epigenetic landscape analysis identifies EPIC1 as an oncogenic lncRNA that interacts with MYC and promotes cell-cycle progression in cancer, Cancer Cell 33 (2018) 706–720, e709.
[22] H. Gu, Y. Xia, L. Guo, Z. Wang, S. Wu, Y. Xu, Y. Zhang, J. Huang, Y. Lei, W. Hu, Long non-coding RNA MILNR1 retards colorectal cancer growth by inhibiting c-Myc, Cancer Commun. (Lond) 40 (2020) 456–460.
[23] O.J. Sansom, V.S. Meniel, V. Muncan, T.J. Phesse, J.A. Wilkins, K.R. Reed, J. K. Vass, D. Athineos, H. Clevers, A.R. Clarke, Myc deletion rescues Apc deficiency in the small intestine, Nature 446 (2007) 676–679.
[24] C. Wang, H. Zou, A. Chen, H. Yang, X. Yu, X. Yu, Y. Wang, C-Myc-activated long non-coding RNA PVT1 enhances the proliferation of cervical cancer cells by sponging miR-486-3p, J. Biochem. 167 (2020) 565–575.

[25] W.L. Hu, L. Jin, A. Xu, Y.F. Wang, R.F. Thorne, X.D. Zhang, M. Wu, GUARDIN is a p53-responsive long non-coding RNA that is essential for genomic stability, Nat. Cell Biol. 20 (2018) 492–502.
[26] M. Martín-Vicente, L.M. Medrano, S. Resino, A. García-Sastre, I. Martínez, TRIM25 in the regulation of the antiviral innate immunity, Front. Immunol. 8 (2017) 1187.
[27] H. Zhou, J.C. Costello, All paths lead to TRIM25, Trends. Cancer 3 (2017) 673–675.
[28] M. Watanabe, S. Hatakeyama, TRIM proteins and diseases, J. Biochem. 161 (2017) 135–144.
[29] P. Malaney, M. Velasco-Estevez, P. Aguilar-Garrido, M.J.L. Aitken, L.E. Chan, X. Zhang, S.M. Post, M. Gallardo, The Eμ-hnRNP K murine model of lymphoma: novel insights into the role of hnRNP K in B-cell malignancies, Front. Immunol. 12 (2021) 634584.
[30] I. Wierstra, J. Alves, The c-myc promoter: still MysterY and challenge, Adv. Cancer Res. 99 (2008) 113–333.
[31] A. Kuzyk, S. Mai, c-MYC-induced genomic instability, Cold. Spring. Harb. Perspect. Med. 4 (2014) a014373.
[32] H. Chen, H. Liu, G. Qing, Targeting oncogenic Myc as a strategy for cancer treatment, Signal. Transduct. Target. Ther. 3 (2018) 5.
[33] M.R. McKeown, J.E. Bradner, Therapeutic strategies to inhibit MYC, Cold. Spring. Harb. Perspect. Med. 4 (2014).
[34] A. Bhan, M. Soleimani, S.S. Mandal, Long noncoding RNA and cancer: a new paradigm, Cancer Res. 77 (2017) 3965–3981.
[35] Z. Wang, H. Qiu, J. He, L. Liu, W. Xue, A. Fox, J. Tickner, J. Xu, The emerging roles of hnRNPK, J. Cell Physiol. 235 (2020), 1995-2008.
[36] D. He, C. Huang, Q. Zhou, D. Liu, L. Xiong, H. Xiang, G. Ma, Z. Zhang, HnRNPK/miR-223/FBXW7 feedback cascade promotes pancreatic cancer cell growth and invasion, Oncotarget. 8 (2017) 20165–20178.
[37] M. Enge, W. Bao, E. Hedström, S.P. Jackson, A. Moumen, G. Selivanova, MDM2-dependent downregulation of p21 and hnRNP K provides a switch between apoptosis and growth arrest induced by pharmacologically activated p53, Cancer Cell 15 (2009) 171–183.
[38] A. Moumen, P. Masterson, M.J. O'Connor, S.P. Jackson, hnRNP K: an HDM2 target and transcriptional coactivator of p53 in response to DNA damage, Cell 123 (2005) 1065–1078.
[39] B. Mucha, S. Qie, S. Bajpai, V. Tarallo, J.N. Diehl, F. Tedeschi, G. Zhou, Z. Gao, S. Flashner, A.J. Klein-Szanto, et al., Tumor suppressor mediated ubiquitylation of hnRNPK is a barrier to oncogenic translation, Nat. Commun. 13 (2022) 6614.
[40] C.J. Huang, C.C. Huang, C.C. Chang, Association of the testis-specific TRIM/RBCC protein RNF33/TRIM60 with the cytoplasmic motor proteins KIF3A and KIF3B, Mol. Cell Biochem. 360 (2012) 121–131.
[41] A.S. Farrell, R.C. Sears, MYC degradation, Cold. Spring. Harb. Perspect. Med. 4 (2014).
[42] G. Hu, Z. Lou, M. Gupta, The long non-coding RNA GAS5 cooperates with the eukaryotic translation initiation factor 4E to regulate c-Myc translation, PLoS. One 9 (2014) e107016.
[43] P. Zhang, L. Cao, P. Fan, Y. Mei, M. Wu, LncRNA-MIF, a c-Myc-activated long non-coding RNA, suppresses glycolysis by promoting Fbxw7-mediated c-Myc degradation, EMBo Rep. 17 (2016) 1204–1220.
[44] M. Gabay, Y. Li, D.W. Felsher, MYC activation is a hallmark of cancer initiation and maintenance, Cold. Spring. Harb. Perspect. Med. 4 (2014).
[45] M. Conacci-Sorrell, L. McFerrin, R.N. Eisenman, An overview of MYC and its interactome, Cold. Spring. Harb. Perspect. Med. 4 (2014) a014357.
[46] B.L. Allen-Petersen, R.C. Sears, Mission possible: advances in MYC therapeutic targeting in cancer, BioDrugs 33 (2019) 539–553.
[47] C. Yan, P.J. Higgins, Drugging the undruggable: transcription therapy for cancer, Biochim. Biophys. Acta 1835 (2013) 76–85.
[48] J.E. Delmore, G.C. Issa, M.E. Lemieux, P.B. Rahl, J. Shi, H.M. Jacobs, E. Kastritis, T. Gilpatrick, R.M. Paranal, J. Qi, et al., BET bromodomain inhibition as a therapeutic strategy to target c-Myc, Cell 146 (2011) 904–917.
[49] M. Toyoshima, H.L. Howie, M. Imakura, R.M. Walsh, J.E. Annis, A.N. Chang, J. Frazier, B.N. Chau, A. Loboda, P.S. Linsley, et al., Functional genomics identifies therapeutic targets for MYC-driven cancer, Proc. Natl. Acad. Sci. u S. a 109 (2012) 9545–9550.
[50] H. Adachi, M. Hengesbach, Y.T. Yu, P. Morais, From antisense RNA to RNA modification: therapeutic potential of RNA-based technologies, Biomedicines. 9 (2021).
[51] C.I.E. Smith, R. Zain, Therapeutic oligonucleotides: state of the art, Annu. Rev. Pharmacol. Toxicol. 59 (2019) 605–630.
[52] G. Kara, G.A. Calin, B. Ozpolat, RNAi-based therapeutics and tumor targeted delivery in cancer, Adv. Drug Deliv. Rev. 182 (2022) 114113.
[53] M.I. Sajid, M. Moazzam, Y. Cho, S. Kato, A. Xu, J.J. Way, S. Lohan, R.K. Tiwari, siRNA therapeutics for the therapy of COVID-19 and other coronaviruses, Mol. Pharm. 18 (2021) 2105–2121.
[54] Q. Li, Y. Wang, S. Wu, Z. Zhou, X. Ding, R. Shi, R.F. Thorne, X.D. Zhang, W. Hu, M. Wu, CircACC1 regulates assembly and activation of AMPK complex under metabolic stress, Cell Metab. 30 (2019) 157–173, e157.
[55] L. Jin, W.L. Hu, C.C. Jiang, J.X. Wang, C.C. Han, P. Chu, L.J. Zhang, R.F. Thorne, J. Wilmott, R.A. Scolyer, et al., MicroRNA-149*, a p53-responsive microRNA, functions as an oncogenic regulator in human melanoma, Proc. Natl. Acad. Sci. u S. a 108 (2011) 15840–15845.
[56] W. Gao, Y. Zhang, H. Luo, M. Niu, X. Zheng, W. Hu, J. Cui, X. Xue, Y. Bo, F. Dai, et al., Targeting SKA3 suppresses the proliferation and chemoresistance of laryngeal squamous cell carcinoma via impairing PLK1-AKT axis-mediated glycolysis, Cell Death. Dis. 11 (2020) 919.
[57] Y.C. Feng, X.Y. Liu, L. Teng, Q. Ji, Y. Wu, J.M. Li, W. Gao, Y.Y. Zhang, T. La, H. Tabatabaee, et al., c-Myc inactivation of p53 through the pan-cancer lncRNA MILIP drives cancer pathogenesis, Nat. Commun. 11 (2020) 4980.
[58] F. Wang, J. Flanagan, N. Su, L.C. Wang, S. Bui, A. Nielson, X. Wu, H.T. Vo, X.J. Ma, Y. Luo, RNAscope: a novel in situ RNA analysis platform for formalin-fixed, paraffin-embedded tissues, J. Mol. Diagn. 14 (2012) 22–29.
[59] L. Zhuang, R.A. Scolyer, C.S. Lee, S.W. McCarthy, W.A. Cooper, X.D. Zhang, J. F. Thompson, P. Hersey, Expression of glucose-regulated stress protein GRP78 is related to progression of melanoma, Histopathology 54 (2009) 462–470.
[60] W. Hu, L. Jin, C.C. Jiang, G.V. Long, R.A. Scolyer, Q. Wu, X.D. Zhang, Y. Mei, M. Wu, AEBP1 upregulation confers acquired resistance to BRAF (V600E) inhibition in melanoma, Cell Death. Dis. 4 (2013) e914.
[61] L. Li, Y. Mao, L. Zhao, L. Li, J. Wu, M. Zhao, W. Du, L. Yu, P. Jiang, p53 regulation of ammonia metabolism through urea cycle controls polyamine biosynthesis, Nature 567 (2019) 253–256.